

Dynamic Metasurface Antennas for Energy Efficient Massive MIMO Uplink Communications

Li You, Jie Xu, George C. Alexandropoulos, Jue Wang, Wenjin Wang,
and Xiqi Gao

Abstract

Future wireless communications are largely inclined to deploy a massive number of antennas at the base stations (BS) by exploiting energy-efficient and environmentally friendly technologies. An emerging technology called dynamic metasurface antennas (DMAs) is promising to realize such massive antenna arrays with reduced physical size, hardware cost, and power consumption. This paper aims to optimize the energy efficiency (EE) performance of DMAs-assisted massive MIMO uplink communications. We propose an algorithmic framework for designing the transmit precoding of each multi-antenna user and the DMAs tuning strategy at the BS to maximize the EE performance, considering the availability of the instantaneous and statistical channel state information (CSI), respectively. Specifically, the proposed framework includes Dinkelbach's transform, alternating optimization, and deterministic equivalent methods. In addition, we obtain a closed-form solution to the optimal transmit signal directions for the statistical CSI case, which simplifies the corresponding transmission design. The numerical results show good convergence performance of our proposed algorithms as well as considerable EE performance gains of the DMAs-assisted massive MIMO uplink communications over the baseline schemes.

Index Terms

Part of this work was submitted to the 2021 IEEE Global Communications Conference (GLOBECOM) [1].

Li You, Jie Xu, Wenjin Wang, and Xiqi Gao are with the National Mobile Communications Research Laboratory, Southeast University, Nanjing 210096, China, and also with the Purple Mountain Laboratories, Nanjing 211100, China (e-mail: liyou@seu.edu.cn; xujie@seu.edu.cn; wangwj@seu.edu.cn; xqgao@seu.edu.cn).

George C. Alexandropoulos is with the Department of Informatics and Telecommunications, National and Kapodistrian University of Athens, Panepistimiopolis Ilissia, 15784 Athens Greece (e-mail: alexandg@di.uoa.gr).

Jue Wang is with School of Information Science and Technology, Nantong University, Nantong 226019, China (e-mail: wangjue@ntu.edu.cn).

Dynamic metasurface antennas (DMAs), energy efficiency, massive MIMO, instantaneous and statistical CSI.

I. INTRODUCTION

Future wireless communications are expected to satisfy very high requirements, such as ultra-low latencies, high spectral efficiency (SE), and high energy efficiency (EE), thus presenting a series of new challenges in the 5G and beyond era [2]. Massive multiple-input multiple-output (MIMO) is a promising method to support such requirements by setting massive numbers of antennas at the base station (BS). This has been proven to significantly increase the throughput of wireless systems [3]. However, It brings a great demand on the radio frequency (RF) chains to realize massive MIMO transmissions by conventional antennas with the fully digital architecture [4], which exposes some problems that cannot be ignored in practice, such as increased fabrication cost [5], high power consumption [6], [7], limited physical size and shape, and deployment restriction [8]. To this end, some works have focused on the design of antennas to effectively implement massive MIMO systems. Recent years witness the increasing interest in an emerging antenna technology named dynamic metasurface antennas (DMAs), which is promising to realize practically massive antenna arrays at the BSs [9].

DMA is a brand-new concept for aperture antenna designs, whose properties can be programmed to adapt to the external environment. The core technology is a kind of resonant, sub-wavelength, and artificial antenna element termed as “metamaterial” [10], [11]. By introducing simplified transceiver hardware, the physical properties of metamaterials (especially the permittivity and permeability) can be reconfigured to show a series of desired characteristics with a tiny amount of power consumption. Taking advantage of this feature, DMAs provide a similar ability of beam tailoring and signal processing as conventional antennas [12]–[15]. In addition, the physical size of metamaterials is commonly smaller than the wavelength, thus the waveguides can accommodate massive antenna elements. Meanwhile, the independent data streams processed by a DMAs-based transceiver is much fewer than the number of metamaterials in the digital domain, which means that DMAs-based transceivers enable a form of hybrid analog/digital (A/D) precoding. Such hybrid precoding allows much fewer RF chains than the number of metamaterials at the BS, thus greatly reducing the hardware cost and power consumption. With the appealing characteristics mentioned above, DMAs are promising to realize low-cost, power-efficient, compact, and dynamic massive MIMO systems.

To appreciate the practical value of DMAs, it is sensible to study their differences compared with some existing technologies. Recently, there is another application of metamaterials proposed for wireless communications named reconfigurable intelligent surfaces (RISs) [16]–[23]. RISs commonly act as passive programmable reflectors installed near BSs or users to realize controllable and reconfigurable propagation environments. They can overcome non-line-of-sight conditions and improve the communication coverage, which is similar to relaying, but without any power amplification and baseband signal processing. Unlike RISs, DMAs usually act as active antennas at BSs and mainly focus on signal processing for the next generation transceivers [9]. In addition, DMAs have the following benefits compared with the conventional antennas with the same number of antenna elements in a fully digital architecture [24]: *i*) DMAs-assisted transmission requires much fewer RF chains than the conventional fully digital architecture; *ii*) the space between metamaterials in DMAs arrays is much smaller than that of conventional antenna elements. Hence, by adopting DMAs instead of conventional antennas, the resulting complexity, power consumption, and hardware cost will be significantly reduced. Moreover, as described above, DMAs-based transceivers provide an ability of hybrid analog/digital (A/D) beamforming. Conventional hybrid A/D beamforming requires numerous phase shifters to connect the antenna elements and RF chains. In contrast, DMAs-based transceivers do not require any additional analog combining circuitries, thus resulting in increased flexibility and reduced power consumption.

Since DMAs can realize low-cost, power-efficient, and compact planar arrays, many studies have been conducted on their application to implement massive MIMO systems in recent years. For example, authors in [25] studied DMAs-assisted spatial multiplexing wireless communications, and demonstrated that DMAs could significantly enhance the capacity in MIMO channels with one or two clusters. Authors in [26] studied the application of DMAs for MIMO orthogonal frequency division modulation (OFDM) receivers with bit-limited analog-to-digital converters (ADCs). The results showed that the DMAs-based receivers with bit-limited ADCs were capable of recovering the OFDM signals accurately. Authors in [27] and [28] respectively investigated the DMAs tuning strategies for the uplink and downlink massive MIMO systems. Although DMAs are promising for MIMO communications, most of the existing works focused on DMAs-based SE optimization, while DMAs-based EE optimization has rarely been explored.

It is worth noting that most of the aforementioned works assumed that the instantaneous channel state information (CSI) is perfectly known for transmission design. DMAs weight

parameters are designed to adapt to the available channel states to improve the communication quality. Thus, with the perfectly known instantaneous CSI, the DMAs-assisted systems can achieve a high capacity gain. However, tuning DMAs via exploiting instantaneous CSI in practical systems is inappropriate and inadvisable due to the following reasons. Firstly, instantaneous CSI can be fast time-varying, which forces DMAs to frequently adjust their properties to keep up with the channel states, thus resulting in significant signaling overhead [29]. Secondly, DMAs are equipped with smart controllers for realizing amplitude or phase tuning [30]. Although the smart controllers operate under a tiny amount of energy, they are still power-consuming when overloaded with continuous operations, i.e., frequent tuning would not be energy efficient for DMAs. Therefore, when channels are fast time-varying, it is more reasonable and feasible to exploit the statistical CSI in DMAs-assisted systems, which varies over larger time scales and results in less power consumption compared to exploiting instantaneous CSI.

Motivated by the above concerns, we aim to study the energy-efficient transmit precoding and DMAs tuning strategies for a single-cell multi-user DMAs-assisted massive MIMO uplink system. The main contributions of this paper are summarized as follows.

- We study the EE maximization problem of the single-cell multi-user DMAs-assisted massive MIMO uplink with instantaneous and statistical CSI, respectively. For both cases, we develop a well-structured and low-complexity algorithm framework for the transmit precoding design and DMAs tuning strategy, including the deterministic equivalent (DE) method, Dinkelbach's transform, and alternating optimization (AO) method.
- For the case where instantaneous CSI is perfectly known, we develop an AO-based optimization framework to alternately update the transmit covariance matrices of multi-antenna users and the DMAs weight matrix at the BS. For the transmit covariance matrices, we apply Dinkelbach's transform to solve the concave-linear fractional problem. For the DMAs weights design, we firstly obtain the weight matrix in a closed form by neglecting its physical structure, and then adopt an alternating minimization algorithm to reconfigure it.
- For the case where statistical CSI is exploited, we develop a similar optimization framework to the instantaneous CSI case. Firstly, we derive an optimal closed-form solution to the transmit signal directions of users. Then, we apply the DE method to asymptotically approximate the ergodic SE to reduce the computational overhead. Next, we adopt Dinkelbach's transform to obtain users' power allocation matrices. Finally, we obtain the DMAs weight matrix with

the same method as the instantaneous CSI case.

- Numerical results show the computational efficiency of our proposed EE optimization framework. Moreover, the conclusion can be drawn that the DMAs-assisted communications can achieve higher EE performance than those based on conventional antennas, especially in the high power budget region.

The rest of the paper is organized as follows: Section II illustrates the DMAs input-output relationship and the channel model. Section III and Section IV investigate the considered EE maximization problem of the DMAs-assisted MIMO uplink communications with instantaneous and statistical CSI, respectively. Section V provides our simulation results. Finally, Section VI concludes this paper.

The notations used throughout the paper are defined as follows. Boldface lower-case letters denote column vectors, e.g., \mathbf{x} , and x_i denotes i th entry of vector \mathbf{x} ; Boldface upper-case letters denote matrices, e.g., \mathbf{M} , and $(\mathbf{M})_{i,j}$ denotes the (i, j) th entry of \mathbf{M} ; The notation $\mathbf{0}$ denotes a zero vector or matrix, and $\mathbf{M} \succeq \mathbf{0}$ denotes a positive semi-definite matrix; The notations \mathcal{X} , \mathbb{C} , and \mathbb{R} denote sets, sets of complex numbers, and sets of real numbers, respectively; The superscripts $(\cdot)^{-1}$, $(\cdot)^H$, and $(\cdot)^T$ represent the matrix inverse, conjugate-transpose, and transpose, respectively; The operators $\text{tr}\{\cdot\}$, $\mathbb{E}\{\cdot\}$, $\text{diag}\{\cdot\}$, and $|\mathbf{M}|$ represent matrix trace, expectation, diagonalization, and determinant of matrix \mathbf{M} , respectively; The operator $\text{Re}(\cdot)$ means to obtain the real part of the input, and the operator $\|\cdot\|_F$ means to obtain Frobenius norm of the input; The operator \odot denotes Hadamard product; The notations j and \mathcal{O} denote the imaginary unit and computational complexity, respectively.

II. SYSTEM MODEL

Our work considers a single-cell massive MIMO uplink system where the BS simultaneously receives signals from multiple users. The BS is equipped with a planar array consisting of metamaterials, and each user is equipped with multiple conventional antennas in a fully digital architecture. In the following, we illustrate the input-output relationship of DMAs and the channel model.

A. Dynamic Metasurface Antennas

As shown in Fig. 1, the considered system is composed of a DMAs-based BS and U users. We define $\mathcal{U} \triangleq \{1, 2, \dots, U\}$ as the user set and N_u as the number of conventional antennas

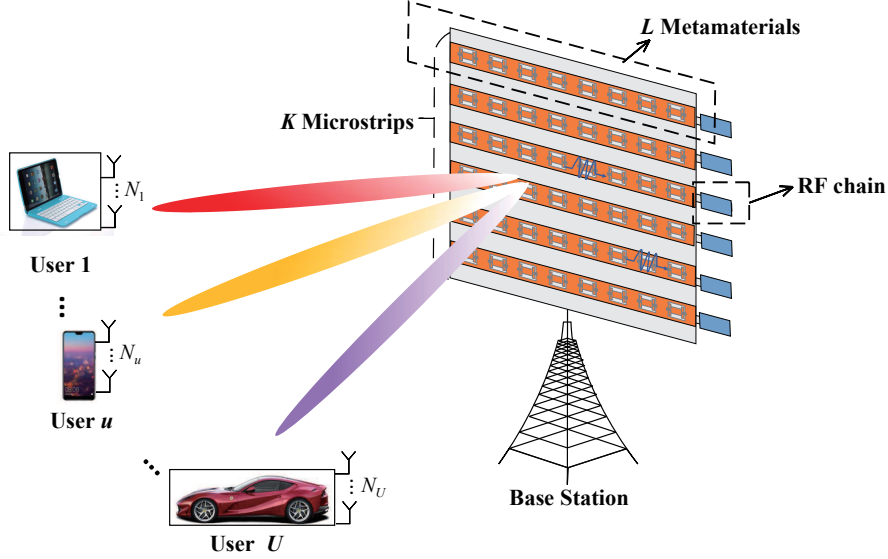


Fig. 1. The considered DMAs-assisted massive MIMO uplink system.

at user $u \in \mathcal{U}$. We assume that the DMAs array consists of K microstrips (e.g., the guiding structure whose top layer is embedded with metamaterials) and each microstrip consists of L metamaterials, i.e., $M = K \times L$. Each metamaterial observes the radiations from the channel, adjusts and transmits them along microstrips to the RF chains independently. The output signal of each microstrip is the linear combination of all the radiation observed by L metamaterials [28].

We denote $\mathbf{y}[i] \in \mathbb{C}^{K \cdot L \times 1}$ as the DMAs input signals where $(\mathbf{y}[i])_{(k-1)L+l}$, $k \in \{1, \dots, K\}$, $l \in \{1, \dots, L\}$ represents the observed radiation of the l th metamaterial in the k th microstrip at time index i . According to [9], such metamaterial element acts as a resonant electrical circuit and can be modeled as a causal filter with a finite impulse response. Hence, we use $\{h_{k,l}[\tau]\}_{\tau=0}^{m_h} \in \mathbb{C}$ to denote such causal filter of the l th metamaterial in the k th microstrip, where m_h is the number of time-delay taps, and use $\mathbf{H}[\tau] \in \mathbb{C}^{M \times M}$ to denote a diagonal matrix where $(\mathbf{H}[\tau])_{(k-1)L+l, (k-1)L+l} = h_{k,l}[\tau]$. Besides, we denote $\mathbf{Q} \in \mathbb{C}^{K \times M}$ as the configurable weight matrix of DMAs and $\mathbf{z}[i] \in \mathbb{C}^{K \times 1}$ as the DMAs output signals at time index i . Here, we consider the case where all the metamaterials have the same frequency selectivity [28], i.e., $\mathbf{H}[\tau] = \mathbf{I}_M \cdot h[\tau]$. Then, the relationship between the DMAs input $\mathbf{y}[i]$ and output $\mathbf{z}[i]$ can be

formulated as

$$\mathbf{z}[i] = \mathbf{Q} \sum_{\tau=0}^{m_h} h[\tau] \mathbf{y}[i - \tau] \in \mathbb{C}^{K \times 1}. \quad (1)$$

We assume that the weight matrix \mathbf{Q} and the frequency selectivity matrix $\mathbf{H}[\tau]$ are independent of each other [28]. In addition, we assume that the metamaterials are weakly coupled and the material-material coupling inside the microstrip can be ignored [15].

In our work, DMAs are tiled as a two-dimensional array, and the weight matrix \mathbf{Q} is formulated as

$$(\mathbf{Q})_{k_1, (k_2-1)L+l} = \begin{cases} q_{k_1, l}, & k_1 = k_2 \\ 0, & k_1 \neq k_2 \end{cases}, \quad (2)$$

where $k_1, k_2 \in \{1, 2, \dots, K\}$, $l \in \{1, 2, \dots, L\}$, and $q_{k_1, l}$ is the gain of the l th metamaterial in the k_1 th microstrip. Eq. (2) considers the fact that the two-dimensional DMAs are formed by tiling together a set of one-dimensional microstrips [28]. Hence, Eq. (2) is referred to as the physical structure constraint of DMAs. Actually, by slightly modifying (2), the input-output relationship of any two-dimensional DMAs can be denoted by (1).

B. Channel Model

We define $\mathbf{x}_u[i] \in \mathbb{C}^{N_u \times 1}$ as the transmit signals from user u at time index i with zero mean and the transmit covariance matrix $\mathbb{E}\{\mathbf{x}_u \mathbf{x}_u^H\} = \mathbf{P}_u \in \mathbb{C}^{N_u \times N_u}$. Additionally, \mathbf{x}_u satisfies $\mathbb{E}\{\mathbf{x}_u \mathbf{x}_{u'}^H\} = \mathbf{0}$, $\forall u \neq u'$, which represents that the input signals from different users are independent of each other. Then, the channel output signals $\mathbf{y}[i]$ at time index i is given by

$$\mathbf{y}[i] = \sum_{u=1}^U \mathbf{G}_u \mathbf{x}_u[i] + \mathbf{n}[i] \in \mathbb{C}^{M \times 1}. \quad (3)$$

In (3), $\mathbf{G}_u \in \mathbb{C}^{M \times N_u}$ denotes the channel between user u and the BS. $\mathbf{n}[i] \in \mathbb{C}^{M \times 1}$ denotes the independently and identically distributed noise at time index i with covariance $\sigma^2 \mathbf{I}_M$, where σ^2 denotes the noise power.

We adopt the jointly-correlated Rayleigh fading channel model, in which the correlation properties at the users and the BS are modeled jointly [31]. Then, the channel matrices \mathbf{G}_u , $\forall u \in \mathcal{U}$, can be formulated as

$$\mathbf{G}_u = \mathbf{U}_u \tilde{\mathbf{G}}_u \mathbf{V}_u^H, \quad \forall u \in \mathcal{U}. \quad (4)$$

In (4), $\mathbf{V}_u \in \mathbb{C}^{N_u \times N_u}$ and $\mathbf{U}_u \in \mathbb{C}^{M \times M}$ are both deterministic unitary matrices, representing the eigenvectors of the transmit and receive correlation matrices, respectively [31]. In addition, $\tilde{\mathbf{G}}_u \in \mathbb{C}^{M \times N_u}$ represents the beam domain channel matrix, whose entries are zero-mean and independently Gaussian distributed. The channel statistics of $\tilde{\mathbf{G}}_u$ can be modeled as

$$\boldsymbol{\Omega}_u = \mathbb{E} \left\{ \tilde{\mathbf{G}}_u \odot \tilde{\mathbf{G}}_u^* \right\} \in \mathbb{R}^{M \times N_u}. \quad (5)$$

In (5), the entry, $[\boldsymbol{\Omega}_u]_{m,n}$, denotes the average energy coupled by the m th column entries of \mathbf{U}_u and the n th column entries of \mathbf{V}_u . Hence, $\boldsymbol{\Omega}_u$ is also named as the eigenmode channel coupling matrix [31].

Since DMAs act as receive antennas at the BS in our considered uplink, they observe and process signals from channels, i.e., channel output signals are fed directly to DMAs. With the input-output relationship of DMAs and the channels given by (1) and (3), respectively, the relationship between the channel input and the DMAs output can be obtained by

$$\mathbf{z}[i] = \sum_{u=1}^U \sum_{\tau=0}^{m_h} \tilde{\mathbf{H}}_u[\tau] \mathbf{x}_u[i - \tau] + \tilde{\mathbf{n}}[i] \in \mathbb{C}^{K \times 1}, \quad (6)$$

where $\tilde{\mathbf{H}}_u[\tau] \triangleq h[\tau] \mathbf{Q} \mathbf{G}_u$ and $\tilde{\mathbf{n}}[i] \triangleq \mathbf{Q} \sum_{\tau=0}^{m_h} h[\tau] \mathbf{n}[i - \tau]$.

III. EE OPTIMIZATION WITH INSTANTANEOUS CSI

In this section, we study the EE optimization of our DMAs-assisted MIMO uplink system via exploiting the instantaneous CSI. We firstly introduce the EE definition of our considered system. Then, we focus on designing the transmit covariance matrices \mathbf{P}_u , $\forall u \in \mathcal{U}$, and the DMAs weight matrix \mathbf{Q} to maximize the system EE performance.

A. Problem Formulation

To define the system EE, we start with the SE definition of the DMAs-assisted uplink system. Based on [28], the achievable instantaneous system SE is given by

$$R = \log_2 \left| \mathbf{I}_K + \frac{1}{\sigma^2} \sum_{u=1}^U \mathbf{Q} \mathbf{G}_u \mathbf{P}_u \mathbf{G}_u^H \mathbf{Q}^H (\mathbf{Q} \mathbf{Q}^H)^{-1} \right|. \quad (7)$$

Under the assumption that all metamaterials have the same frequency selectivity, $\mathbf{H}[\tau]$ is expressed as \mathbf{I} multiplied by a constant, thus $\mathbf{H}[\tau]$ is eliminated in (7).

The whole power consumption of the DMAs-assisted system consists of three major parts, including the transmit power, static hardware power, and dynamic power. Referring to [17], [25], the whole power consumption of our DMAs-assisted system is given by

$$W = \sum_{u=1}^U (\xi_u \text{tr} \{\mathbf{P}_u\} + W_{c,u}) + W_{\text{BS}} + KW_S. \quad (8)$$

In (8), $\xi_u = \rho_u^{-1}$ where ρ_u denotes the transmit power amplifier efficiency of user u . $\text{tr} \{\mathbf{P}_u\}$ and $W_{c,u}$ denote the transmit power consumption and static circuit power dissipation of user u , respectively. W_S represents the dynamic power dissipation of each RF chain (e.g., power consumption in the ADCs, amplifier, and mixer). W_{BS} incorporates the static circuit power dissipation at the BS. Note that the conventional antennas with a fully digital architecture require as many RF chains as the antenna elements. However, the DMAs array only requires as few RF chains as microstrips, resulting in the reduced dynamic power consumption by a factor of L [25]. In addition, the hybrid A/D architecture with conventional antennas also allows a reduced demand on RF chains. But it requires additional power consumption to support the phase shifters and switches.

With the system SE in (7) and power consumption in (8), the EE of our DMAs-assisted uplink system is given by

$$EE = B \cdot \frac{R}{W}, \quad (9)$$

where B is a constant denoting the channel bandwidth.

So far, the EE maximization problem of the DMAs-assisted uplink system by designing the transmit covariance matrices \mathbf{P}_u , $\forall u$, and DMAs weight matrix \mathbf{Q} is formulated as follows:

$$\mathcal{P}_1 : \max_{\mathbf{Q}, \mathbf{P}} \frac{\log_2 \left| \mathbf{I}_K + \frac{1}{\sigma^2} \sum_{u=1}^U \mathbf{Q} \mathbf{G}_u \mathbf{P}_u \mathbf{G}_u^H \mathbf{Q}^H (\mathbf{Q} \mathbf{Q}^H)^{-1} \right|}{\sum_{u=1}^U (\xi_u \text{tr} \{\mathbf{P}_u\} + W_{c,u}) + W_{\text{BS}} + KW_S} \quad (10a)$$

$$\text{s.t.} \quad (\mathbf{Q})_{k_1, (k_2-1)L+l} = \begin{cases} q_{k_1, l}, & k_1 = k_2 \\ 0, & k_1 \neq k_2 \end{cases}, \quad (10b)$$

$$\text{tr} \{\mathbf{P}_u\} \leq P_{\max}, \quad \mathbf{P}_u \succeq \mathbf{0}, \quad \forall u \in \mathcal{U}, \quad (10c)$$

where P_{\max} denotes the maximum available transmit power. In addition, $\mathbf{P} \triangleq \{\mathbf{P}_1, \mathbf{P}_2, \dots, \mathbf{P}_U\}$,

$k_1, k_2 \in \{1, 2, \dots, K\}$, $l \in \{1, 2, \dots, L\}$. In (10a), we ignore the constant B without loss of generality. Problem \mathcal{P}_1 is challenging to tackle with due to the following reasons. Firstly, since the objective function in (10a) exhibits a fractional form, \mathcal{P}_1 is an NP-hard problem [32]. Secondly, the structure constraint of \mathbf{Q} in (10b) is non-convex, which further complicates \mathcal{P}_1 . Thirdly, since variables \mathbf{P} and \mathbf{Q} are nonlinearly coupled, it is complicated to design \mathbf{P} and \mathbf{Q} simultaneously. To simplify the optimization process, we adopt an AO method to design \mathbf{P} and \mathbf{Q} in an alternating manner. For the optimization of \mathbf{P} , we adopt Dinkelbach's transform to convert the concave-linear fraction in (10a) into a concave one. For the optimization of \mathbf{Q} , we first neglect constraint (10b) to obtain the corresponding unconstrained \mathbf{Q} , and then adopt an alternating minimization algorithm to reconfigure \mathbf{Q} constrained by (10b). Note that when ξ_u , $\forall u \in \mathcal{U}$, in (10a) is equal to zero, the denominator of the objective function is converted to a constant, and \mathcal{P}_1 is reduced into a SE optimization problem. Thus, problem \mathcal{P}_1 can describe both the EE and SE maximization problems of the considered DMAs-assisted uplink communications.

B. Optimization of the Unconstrained Weight Matrix

When optimizing \mathbf{Q} with an arbitrarily given \mathbf{P} , the denominator of (10a) can be treated as a constant. Thus, we only need to focus on the numerator of (10a). By defining $\bar{\mathbf{G}} = \frac{1}{\sigma^2} \sum_{u=1}^U \mathbf{G}_u \mathbf{P}_u \mathbf{G}_u^H$, and applying Sylvester's determinant identity $\log_2 |\mathbf{I} + \mathbf{A}\mathbf{B}| = \log_2 |\mathbf{I} + \mathbf{B}\mathbf{A}|$, the numerator of (10a) can be written as

$$R = \log_2 \left| \mathbf{I}_M + \bar{\mathbf{G}} \mathbf{Q} \mathbf{Q}^H (\mathbf{Q} \mathbf{Q}^H)^{-1} \mathbf{Q} \right|. \quad (11)$$

Let $\bar{\mathbf{V}}_1$ denote the right singular vectors matrix of \mathbf{Q} , and $\bar{\mathbf{V}}_2$ denote the first K columns of $\bar{\mathbf{V}}_1$. According to the projection matrix property that $\mathbf{Q}^H (\mathbf{Q} \mathbf{Q}^H)^{-1} \mathbf{Q} = \bar{\mathbf{V}}_2 \bar{\mathbf{V}}_2^H$ [33], Eq. (11) can be written as

$$R = \log_2 \left| \mathbf{I}_K + \bar{\mathbf{V}}_2^H \bar{\mathbf{G}} \bar{\mathbf{V}}_2 \right|. \quad (12)$$

With the non-convex constraint (10b), Eq. (12) is difficult to tackle directly. Hence, we drop constraint (10b) and consider a relaxed version of problem \mathcal{P}_1 . Then, when designing \mathbf{Q} with a given \mathbf{P} , problem \mathcal{P}_1 is recast as follows

$$\mathcal{P}_2 : \quad \max_{\bar{\mathbf{V}}_2} \log_2 \left| \mathbf{I}_K + \bar{\mathbf{V}}_2^H \bar{\mathbf{G}} \bar{\mathbf{V}}_2 \right|. \quad (13)$$

The solution to \mathcal{P}_2 can be obtained in a close form according to *Proposition 1*, as follows.

Proposition 1: Let $\bar{\mathbf{V}}_3$ denote the eigenvectors corresponding to the largest K eigenvalues of $\bar{\mathbf{G}}$. Then, the maximal achievable SE in (13) can be achieved by setting $\bar{\mathbf{V}}_2$ as $\bar{\mathbf{V}}_3$, i.e.,

$$\bar{\mathbf{V}}_2 = \bar{\mathbf{V}}_3. \quad (14)$$

The proof of *Proposition 1* is similar to [28, Corollary 2], thus is omitted here.

By the singular value decomposition (SVD), the DMAs weight matrix \mathbf{Q} can be written as

$$\mathbf{Q} = \bar{\mathbf{U}}_2 \bar{\mathbf{D}}_2 \bar{\mathbf{V}}_2^H, \quad (15)$$

where $\bar{\mathbf{U}}_2 \in \mathbb{C}^{K \times K}$ and $\bar{\mathbf{D}}_2 \in \mathbb{C}^{K \times K}$ denote the left singular matrix and the diagonal singular value matrix of \mathbf{Q} , respectively. From *Proposition 1*, we can find that the maximal SE in (11) only depends on the right singular matrix $\bar{\mathbf{V}}_2$ and is independent of $\bar{\mathbf{U}}_2$ and $\bar{\mathbf{D}}_2$. Thus, we can design $\bar{\mathbf{U}}_2$ and $\bar{\mathbf{D}}_2$ to obtain \mathbf{Q} with constraint (10b).

C. Optimization of the Transmit Covariance Matrices

When designing the transmit covariance matrices $\mathbf{P}_u, \forall u \in \mathcal{U}$, with a given $\bar{\mathbf{V}}_2$, problem \mathcal{P}_1 is recast as

$$\mathcal{P}_3 : \quad \max_{\mathbf{P}} \quad \frac{\log_2 \left| \mathbf{I}_K + \frac{1}{\sigma^2} \sum_{u=1}^U \bar{\mathbf{V}}_2^H \mathbf{G}_u \mathbf{P}_u \mathbf{G}_u^H \bar{\mathbf{V}}_2 \right|}{\sum_{u=1}^U (\xi_u \text{tr} \{ \mathbf{P}_u \} + W_{c,u}) + W_{\text{BS}} + MW_S}, \quad (16a)$$

$$\text{s.t.} \quad \text{tr} \{ \mathbf{P}_u \} \leq P_{\max}, \quad \mathbf{P}_u \succeq \mathbf{0}, \quad \forall u \in \mathcal{U}. \quad (16b)$$

Eq. (16a) is a concave-linear fraction, whose numerator is concave and denominator is linear with respect to $\mathbf{P}_u, \forall u$. Dinkelbach's transform is a classical method to tackle with this kind of problems, and is guaranteed to converge to the optimal solutions to \mathcal{P}_3 with a super-linear rate [32]. By invoking Dinkelbach's transform, problem \mathcal{P}_3 is transformed to

$$\mathcal{P}_4 : \quad \arg \max_{\mathbf{P}, \eta_1} \quad R(\mathbf{P}) - \eta_1 W(\mathbf{P}), \quad (17a)$$

$$\text{s.t.} \quad \text{tr} \{ \mathbf{P}_u \} \leq P_{\max}, \quad \mathbf{P}_u \succeq \mathbf{0}, \quad \forall u \in \mathcal{U}. \quad (17b)$$

In \mathcal{P}_4 , $R(\mathbf{P})$ and $W(\mathbf{P})$ respectively denote the numerator and denominator of (16a), and η_1 is an auxiliary variable. Problem \mathcal{P}_4 can be addressed by alternatingly optimizing \mathbf{P} and η_1 .

With an arbitrarily given η_1 , the optimal \mathbf{P} can be obtained by classical convex optimization techniques [34]. With an arbitrarily given \mathbf{P} , the optimal η_1 is obtained by

$$\eta_1^* = \frac{R(\mathbf{P})}{W(\mathbf{P})}. \quad (18)$$

More details about the procedure based on Dinkelbach's transform are summarized in **Algorithm 1**.

Algorithm 1 Dinkelbach's Transform

Input: The right singular matrix $\bar{\mathbf{V}}_2$, threshold ϵ .

1: Initialize $\eta_1^{(\ell)}$ and set iteration index $\ell = 0$.

2: **repeat**

3: $\ell \leftarrow \ell + 1$.

4: Calculate $\mathbf{P}^{(\ell)}$ in (17) with $\eta_1^{(\ell-1)}$.

5: Calculate $\eta_1^{(\ell)}$ in (18) with $\mathbf{P}^{(\ell)}$.

6: **until** $|\eta_1^{(\ell)} - \eta_1^{(\ell-1)}| \leq \epsilon$

Output: The optimal transmit covariance matrices $\mathbf{P} = \mathbf{P}^{(\ell)}$.

D. Optimization of the Constrained Weight Matrix

As is illustrated in Subsection III-B, the maximal SE of \mathcal{P}_2 is independent of the unitary matrix $\bar{\mathbf{U}}_2$ and diagonal matrix $\bar{\mathbf{D}}_2$. Referring to [28], we adopt an alternating minimization algorithm to adjust $\bar{\mathbf{U}}_2$, $\bar{\mathbf{D}}_2$, and \mathbf{Q} . Let $\mathcal{Q}_2^{K \times M}$ denote the set of $K \times M$ matrices which conforms to (10b), \mathcal{U}^K denote the set of $K \times K$ unitary matrices, and \mathcal{D}^K denote the set of $K \times K$ diagonal matrices with positive diagonal entries. The corresponding alternating approximation problem is given by

$$\mathcal{P}_5 : \min_{\mathbf{Q} \in \mathcal{Q}_2^{K \times M}, \bar{\mathbf{U}}_2 \in \mathcal{U}^K, \bar{\mathbf{D}}_2 \in \mathcal{D}^K} \|\mathbf{Q} - \bar{\mathbf{U}}_2 \bar{\mathbf{D}}_2 \bar{\mathbf{V}}_3^H\|_{\text{F}}^2. \quad (19)$$

The detailed calculation of \mathbf{Q} , $\bar{\mathbf{U}}_2$, and $\bar{\mathbf{D}}_2$ are described as follows.

Firstly, we define $\mathbf{M} \triangleq \bar{\mathbf{U}}_2 \bar{\mathbf{D}}_2 \bar{\mathbf{V}}_3^H$. By designing \mathbf{Q} with arbitrarily given $\bar{\mathbf{U}}_2$ and $\bar{\mathbf{D}}_2$, we have that

$$\mathbf{Q}^{\text{AM}}(\mathbf{M}) \triangleq \arg \min_{\mathbf{Q} \in \mathcal{Q}_2^{K \times M}} \|\mathbf{Q} - \mathbf{M}\|_{\text{F}}^2. \quad (20a)$$

By defining \mathcal{Q} as the set of possible values for the entries of \mathbf{Q} , we have

$$(\mathbf{Q}^{\text{AM}}(\mathbf{M}))_{k_1, (k_2-1)L+l} = \begin{cases} \arg \min_{q \in \mathcal{Q}} |q - (\mathbf{M})_{k_1, (k_2-1)L+l}|^2, & k_1 = k_2 \\ 0, & k_1 \neq k_2 \end{cases}. \quad (20b)$$

Secondly, we define $\mathbf{M}_1 = \mathbf{Q}$ and $\mathbf{M}_2 = \bar{\mathbf{D}}_2 \bar{\mathbf{V}}_3^H$. By letting $\bar{\mathbf{U}}$ and $\tilde{\mathbf{V}}$ be the left and right singular vector matrices of $\mathbf{M}_1 \mathbf{M}_2^H$, respectively, we can obtain $\bar{\mathbf{U}}_2$ with arbitrarily given $\bar{\mathbf{D}}_2$ and \mathbf{Q} via

$$\bar{\mathbf{U}}_2^{\text{AM}}(\mathbf{M}_1, \mathbf{M}_2) \triangleq \arg \min_{\bar{\mathbf{U}}_2 \in \mathcal{U}^K} \|\mathbf{M}_1 - \bar{\mathbf{U}}_2 \mathbf{M}_2\|_{\text{F}}^2 = \tilde{\mathbf{U}} \tilde{\mathbf{V}}^H. \quad (20c)$$

Finally, we define $\mathbf{M}_1 = \bar{\mathbf{U}}_2^H \mathbf{Q}$ and $\mathbf{M}_2 = \bar{\mathbf{V}}_3^H$. By letting $\mathbf{m}_{1,i}$ and $\mathbf{m}_{2,i}$ denote the i th columns of $\bar{\mathbf{M}}_1^H$ and $\bar{\mathbf{M}}_2^H$, respectively, we can obtain $\bar{\mathbf{D}}_2$ with arbitrarily given $\bar{\mathbf{U}}_2$ and \mathbf{Q} via

$$\bar{\mathbf{D}}_2^{\text{AM}}(\mathbf{M}_1, \mathbf{M}_2) \triangleq \arg \min_{\bar{\mathbf{D}}_2 \in \mathcal{D}^K} \|\mathbf{M}_1 - \bar{\mathbf{D}}_2 \mathbf{M}_2\|_{\text{F}}^2. \quad (20d)$$

In (20d), the diagonal entries of $\bar{\mathbf{D}}_2^{\text{AM}}$ are given by

$$(\bar{\mathbf{D}}_2^{\text{AM}}(\mathbf{M}_1, \mathbf{M}_2))_{i,i} = \max \left(\frac{\text{Re}(\mathbf{m}_{1,i}^H, \mathbf{m}_{2,i})}{\|\mathbf{m}_{2,i}\|_{\text{F}}^2}, \delta \right), \quad (20e)$$

where δ is a small positive number [28].

Problem \mathcal{P}_5 can be addressed by alternately calculating (20b), (20c), and (20e). The alternating minimization algorithm for DMAs weight design is summarized in **Algorithm 2**.

Algorithm 2 Alternating Minimization for the DMAs Weights

Input: The right singular matrix $\bar{\mathbf{V}}_3$, threshold ϵ .

- 1: Initialize the iteration index $\ell = 0$, $\bar{\mathbf{U}}_2^{(\ell)} = \mathbf{I}_K$ and $\bar{\mathbf{D}}_2^{(\ell)} = \mathbf{I}_K$.
- 2: **repeat**
- 3: Set $\ell = \ell + 1$.
- 4: Set $\mathbf{Q}^{(\ell)} = \mathbf{Q}^{\text{AM}}$ with $\mathbf{M} = \bar{\mathbf{U}}_2^{(\ell-1)} \bar{\mathbf{D}}_2^{(\ell-1)} \bar{\mathbf{V}}_3^H$ using (20b).
- 5: Set $\bar{\mathbf{U}}_2^{(\ell)} = \bar{\mathbf{U}}_2^{\text{AM}}$ with $\mathbf{M}_1 = \mathbf{Q}^{(\ell)}$ and $\mathbf{M}_2 = \bar{\mathbf{D}}_2^{(\ell-1)} \bar{\mathbf{V}}_3^H$ using (20c).
- 6: Set $\bar{\mathbf{D}}_2^{(\ell)} = \bar{\mathbf{D}}_2^{\text{AM}}$ with $\mathbf{M}_1 = (\bar{\mathbf{U}}_2^{(\ell)})^H \mathbf{Q}^{(\ell)}$ and $\mathbf{M}_2 = \bar{\mathbf{V}}_3^H$ using (20e).
- 7: **until** $\|\mathbf{Q}^{(\ell)} - \mathbf{Q}^{(\ell-1)}\|_{\text{F}} \leq \epsilon$

Output: The weight matrix $\mathbf{Q} = \mathbf{Q}^{(\ell)}$.

E. Overall Algorithm and Complexity Analysis

So far, we have studied the EE maximization problem \mathcal{P}_1 of the DMAs-assisted MIMO uplink communications with instantaneous CSI. The approaches for designing users' transmit covariance matrices and the DMAs weight matrix were described in Subsection III-B, Subsection III-C and Subsection III-D, respectively. Now, we present the complete AO-based algorithm to find the transmit covariance matrices and the DMAs weight matrix in **Algorithm 3**.

The main structure of the **Algorithm 3** includes an AO method (i.e., alternately designing \mathbf{P} in \mathcal{P}_4 and the unconstrained $\bar{\mathbf{V}}_2$ in \mathcal{P}_2) and **Algorithm 2** (i.e., alternately designing constrained \mathbf{Q} , $\bar{\mathbf{U}}_2$ and $\bar{\mathbf{D}}_2$ in \mathcal{P}_5). We assume that the AO method converges after I_{AO} iterations and **Algorithm 2** converges after I_C iterations. Firstly, we discuss the complexity of the AO-based algorithm for optimizing \mathbf{P} and unconstrained $\bar{\mathbf{V}}_2$. For the transmit covariance matrices \mathbf{P} optimized by Dinkelbach's method, we assume that the optimization process requires I_{DK1} iterations. Since each iteration needs to optimize $\sum_{u=1}^U N_u^2$ variables and the complexity per iteration is polynomial over the number of variables [35], the complexity of optimizing the transmit covariance matrices \mathbf{P} is estimated as $\mathcal{O}(I_{\text{DK1}}(\sum_{u=1}^U N_u^2)^p)$, where $1 \leq p \leq 4$ [19]. For optimizing $\bar{\mathbf{V}}_2$ in problem \mathcal{P}_2 , it requires one iteration and the computational complexity mainly depends on the eigenvalue decomposition of $\frac{1}{\sigma^2} \mathbf{G}_u \mathbf{P}_u \mathbf{G}_u^H$, which concludes $M \times M$ variables. Thus, the complexity of optimizing $\bar{\mathbf{V}}_2$ is estimated as $\mathcal{O}(M^3)$, which is small and negligible compared with the complexity of optimizing \mathbf{P} . Therefore, the complexity of the AO-based algorithm for optimizing \mathbf{P} and unconstrained $\bar{\mathbf{V}}_2$ is estimated as $\mathcal{O}(I_{\text{AO}} I_{\text{DK1}} (\sum_{u=1}^U N_u^2)^p)$. Then, for **Algorithm 2**, the computational complexity per iteration depends on the complexity of calculating \mathbf{Q} , $\bar{\mathbf{U}}_2$, and $\bar{\mathbf{D}}_2$ in (20b), (20c) and (20e), respectively, which is estimated as $\mathcal{O}(M^3)$. Hence, with the assumption that **Algorithm 2** requires I_C iterations, the complexity of **Algorithm 2** can be estimated as $\mathcal{O}(I_C M^3)$. Therefore, the computational complexity of the proposed EE maximization algorithm for the considered DMAs-assisted MIMO uplink with instantaneous CSI is estimated as $\mathcal{O}(I_{\text{AO}} I_{\text{DK1}} (\sum_{u=1}^U N_u^2)^p + I_C M^3)$.

IV. EE OPTIMIZATION WITH STATISTICAL CSI

Channels might be fast time-varying in practical wireless communications, thus frequently tuning DMAs and reallocating transmit power with instantaneous CSI is difficult. In such cases, utilizing the statistical CSI to optimize the system EE performance is more efficient [31]. In this

Algorithm 3 AO-based Algorithm for EE Maximization with Instantaneous CSI

Input: The channel matrices $\mathbf{G}_u, \forall u$, the noise power σ^2 , power consumptions $W_{c,u}, W_{BS}$, and W_S , threshold ϵ .

- 1: Initialize the iteration index $\ell = 0$, the unconstrained right singular matrix $\bar{\mathbf{V}}_2^{(\ell)}$, and the EE performance $EE^{(\ell)}$.
- 2: **repeat**
- 3: $\ell = \ell + 1$.
- 4: Obtain $\mathbf{P}_u^{(\ell)}, \forall u$, with $\bar{\mathbf{V}}_2^{(\ell-1)}$ and **Algorithm 1**.
- 5: Obtain $\bar{\mathbf{V}}_2^{(\ell)}$ with $\mathbf{P}_u^{(\ell)}, \forall u$, and *Proposition 1*.
- 6: Update $EE^{(\ell)}$ using $\mathbf{P}_u^{(\ell)}, \forall u$, and $\bar{\mathbf{V}}_2^{(\ell)}$.
- 7: **until** $|EE^{(\ell)} - EE^{(\ell-1)}| \leq \epsilon$
- 8: Obtain the weight matrix \mathbf{Q} with $\bar{\mathbf{V}}_2^{(\ell)}$ and **Algorithm 2**.

Output: The weight matrix \mathbf{Q} and the transmit covariance matrices $\mathbf{P}_u = \mathbf{P}_u^{(\ell)}, \forall u$.

section, we explore approaches to optimize the system EE by designing the transmit covariance matrices and DMAs weight matrix via exploiting statistical CSI.

A. Problem Formulation

To formulate the corresponding EE maximization problem, we firstly describe the system SE and power consumption metrics. For the statistical CSI case, we adopt the ergodic achievable SE metric defined as:

$$\bar{R} = \mathbb{E} \left\{ \log_2 \left| \mathbf{I}_K + \frac{1}{\sigma^2} \sum_{u=1}^U \mathbf{Q} \mathbf{G}_u \mathbf{P}_u \mathbf{G}_u^H \mathbf{Q}^H (\mathbf{Q} \mathbf{Q}^H)^{-1} \right| \right\}, \quad (21)$$

where the expectation is taken over the channel realizations.

In addition, we use (8) to represent the overall power consumption. Then, the corresponding EE maximization problem can be formulated as

$$\bar{\mathcal{P}}_1 : \max_{\mathbf{Q}, \mathbf{P}} \frac{\mathbb{E} \left\{ \log_2 \left| \mathbf{I}_K + \frac{1}{\sigma^2} \sum_{u=1}^U \mathbf{Q} \mathbf{G}_u \mathbf{P}_u \mathbf{G}_u^H \mathbf{Q}^H (\mathbf{Q} \mathbf{Q}^H)^{-1} \right| \right\}}{\sum_{u=1}^U (\xi_u \text{tr} \{ \mathbf{P}_u \} + W_{c,u}) + W_{BS} + K W_S}, \quad (22a)$$

$$\text{s.t.} \quad (\mathbf{Q})_{k_1, (k_2-1)L+l} = \begin{cases} q_{k_1, l}, & k_1 = k_2 \\ 0, & k_1 \neq k_2 \end{cases}, \quad (22b)$$

$$\text{tr} \{ \mathbf{P}_u \} \leq P_{\max}, \quad \mathbf{P}_u \succeq \mathbf{0}, \quad \forall u \in \mathcal{U}, \quad (22c)$$

where $k_1, k_2 \in \{1, 2, \dots, K\}$ and $l \in \{1, 2, \dots, L\}$. Note that in problem $\bar{\mathcal{P}}_1$, we utilize the same power consumption notations $W_{c,u}$, W_{BS} , and W_S as those in the instantaneous CSI case. As they are all constants, they will not affect the following optimization development. $\bar{\mathcal{P}}_1$ is challenging to tackle because (22a) exhibits a concave-linear fractional structure and (22b) is a non-convex constraint. In addition, the expectation operation in (22a) further increases the computational overhead. In the following, we aim to cope with the foregoing difficulties for handling the EE optimization problem in $\bar{\mathcal{P}}_1$. Note that when $\xi_u, \forall u \in \mathcal{U}$, is set as zero, problem $\bar{\mathcal{P}}_1$ reduces to a SE optimization problem with statistical CSI.

B. Optimization of Users' Transmit Covariance Matrices

In order to find \mathbf{P} which maximizes (22a), We apply the projection matrix property [33]. Then, the ergodic achievable SE in (21) can be reformulated as

$$\bar{R} = \mathbb{E} \left\{ \log_2 \left| \mathbf{I}_K + \frac{1}{\sigma^2} \sum_{u=1}^U \bar{\mathbf{V}}_2^H \mathbf{G}_u \mathbf{P}_u \mathbf{G}_u^H \bar{\mathbf{V}}_2 \right| \right\}, \quad (23)$$

where $\bar{\mathbf{V}}_2$ denotes the first K columns of the right singular vector matrix of \mathbf{Q} . Similar to Section III, we adopt an AO method to optimize \mathbf{P} and $\bar{\mathbf{V}}_2$ separately. We firstly consider the design of $\mathbf{P}_u, \forall u \in \mathcal{U}$, with an arbitrarily given $\bar{\mathbf{V}}_2$. Then, problem $\bar{\mathcal{P}}_1$ is recast as

$$\bar{\mathcal{P}}_2 : \quad \max_{\mathbf{P}} \quad \frac{\mathbb{E} \left\{ \log_2 \left| \mathbf{I}_K + \frac{1}{\sigma^2} \sum_{u=1}^U \bar{\mathbf{V}}_2^H \mathbf{G}_u \mathbf{P}_u \mathbf{G}_u^H \bar{\mathbf{V}}_2 \right| \right\}}{\sum_{u=1}^U (\xi_u \text{tr} \{ \mathbf{P}_u \} + W_{c,u}) + W_{BS} + KW_S}, \quad (24a)$$

$$\text{s.t.} \quad \text{tr} \{ \mathbf{P}_u \} \leq P_{\max}, \quad \mathbf{P}_u \succeq \mathbf{0}, \quad \forall u \in \mathcal{U}. \quad (24b)$$

Considering the high computational complexity of a large number of variables in $\bar{\mathcal{P}}_2$, we decompose the transmit covariance matrices $\mathbf{P}_u, \forall u \in \mathcal{U}$, into two parts via eigenvalue decomposition, which is written as

$$\mathbf{P}_u = \Phi_u \Lambda_u \Phi_u^H, \quad \forall u \in \mathcal{U}. \quad (25)$$

In (25), Φ_u and Λ_u denote the transmit signal directions and the transmit power allocation of user u , respectively. We will respectively introduce the approaches for Φ_u and $\Lambda_u, \forall u \in \mathcal{U}$, in the following.

1) *Optimal Transmit Directions at Users:* The optimal transmit signal directions can be obtained by the following proposition.

Proposition 2: The optimal transmit direction of user u is identical to the eigenvector matrix of the transmit correlation matrix corresponding to the channel between user u and the BS, i.e.,

$$\Phi_u = \mathbf{V}_u. \quad (26)$$

The proof of *Proposition 2* is similar to [36, Proposition 1], thus is omitted here.

Proposition 2 indicates that the transmit precoding is aligned to the eigenvectors of the transmit correlation matrices to maximize the system EE. By applying *Proposition 2*, the transmit covariance matrix of user u is formulated as $\mathbf{P}_u = \mathbf{V}_u \Lambda_u \mathbf{V}_u^H$, $\forall u \in \mathcal{U}$. Then, problem $\bar{\mathcal{P}}_2$ is formulated as

$$\bar{\mathcal{P}}_3 : \quad \max_{\Lambda} \quad \frac{\mathbb{E} \left\{ \log_2 \left| \mathbf{I}_K + \frac{1}{\sigma^2} \sum_{u=1}^U \bar{\mathbf{V}}_2^H \mathbf{U}_u \tilde{\mathbf{G}}_u \Lambda_u \tilde{\mathbf{G}}_u^H \mathbf{U}_u^H \bar{\mathbf{V}}_2 \right| \right\}}{\sum_{u=1}^U (\xi_u \text{tr} \{ \Lambda_u \} + W_{c,u}) + W_{\text{BS}} + KW_S}, \quad (27a)$$

$$\text{s.t.} \quad \text{tr} \{ \Lambda_u \} \leq P_{\max}, \quad \Lambda_u \succeq \mathbf{0}, \quad \Lambda_u \text{ diagonal}, \quad \forall u \in \mathcal{U}, \quad (27b)$$

where $\Lambda \triangleq \{ \Lambda_1, \Lambda_2, \dots, \Lambda_U \}$. Since the transmit direction, $\Phi_u, \forall u$, can be determined with a closed-form solution by *Proposition 2*, the number of optimization variables has been significantly reduced.

2) *Deterministic Equivalent Method:* Problem $\bar{\mathcal{P}}_3$ can be approximated by the Monte-Carlo method via averaging over a large number of samples, but this method is computationally expensive. Hence, we adopt the DE method, an asymptotic expression based on the large-dimensional random matrix theory, to approximate the expectation in (27a). Define $\hat{\mathbf{G}}_u \triangleq \hat{\mathbf{U}}_u \tilde{\mathbf{G}}_u \hat{\mathbf{V}}_u^H \in \mathbb{C}^{K \times N_u}$, where $\hat{\mathbf{U}}_u \triangleq \bar{\mathbf{V}}_2^H \mathbf{U}_u \in \mathbb{C}^{K \times M}$, $\hat{\mathbf{V}}_u \triangleq \mathbf{I}_{N_u}$, and $\tilde{\mathbf{G}}_u$ denotes the beam domain channel between user u and the BS. Define $\hat{\mathbf{G}} \triangleq [\hat{\mathbf{G}}_1, \hat{\mathbf{G}}_2, \dots, \hat{\mathbf{G}}_U] \in \mathbb{C}^{K \times N}$ and $\mathbf{D} \triangleq \text{diag} \{ \Lambda_1, \Lambda_2, \dots, \Lambda_U \} \in \mathbb{C}^{N \times N}$. Then, the numerator of (27a) is written as

$$\bar{R} = \mathbb{E} \left\{ \log_2 \left| \mathbf{I}_K + \frac{1}{\sigma^2} \hat{\mathbf{G}} \mathbf{D} \hat{\mathbf{G}}^H \right| \right\}. \quad (28)$$

By adopting the DE method [37], Eq. (28) can be approximated by

$$R_{\text{DE}} = \sum_{u=1}^U \log_2 |\mathbf{I}_{N_u} + \Xi_u \Lambda_u| + \log_2 |\mathbf{I}_K + \Psi| - \frac{1}{\ln 2} \sum_{u=1}^U \gamma_u^T \Omega_u \psi_u, \quad (29)$$

where $\boldsymbol{\gamma}_u \triangleq [\gamma_{u,1}, \gamma_{u,2}, \dots, \gamma_{u,M}]^T$, $\boldsymbol{\psi}_u \triangleq [\psi_{u,1}, \psi_{u,2}, \dots, \psi_{u,N_u}]^T$ and $\boldsymbol{\Psi} \triangleq \sum_{u=1}^U \boldsymbol{\Psi}_u \in \mathbb{C}^{K \times K}$. The calculation of $\boldsymbol{\Xi}_u$ and $\boldsymbol{\Psi}_u$, $\forall u \in \mathcal{U}$, are given by

$$\begin{cases} \boldsymbol{\Xi}_u = \widehat{\mathbf{V}}_u \text{diag} \{ \boldsymbol{\Omega}_u^T \boldsymbol{\gamma}_u \} \widehat{\mathbf{V}}_u^H \in \mathbb{C}^{N_u \times N_u}, \\ \boldsymbol{\Psi}_u = \frac{1}{\sigma^2} \widehat{\mathbf{U}}_u \text{diag} \{ \boldsymbol{\Omega}_u \boldsymbol{\psi}_u \} \widehat{\mathbf{U}}_u^H \in \mathbb{C}^{K \times K}. \end{cases} \quad (30)$$

The quantities $\boldsymbol{\gamma} \triangleq \{\gamma_{u,m}\}_{\forall u,m}$ and $\boldsymbol{\psi} \triangleq \{\psi_{u,n}\}_{\forall u,n}$ form the unique solution to the equations

$$\begin{cases} \gamma_{u,m} = \frac{1}{\sigma^2} \widehat{\mathbf{u}}_{u,m}^H (\mathbf{I}_K + \boldsymbol{\Psi})^{-1} \widehat{\mathbf{u}}_{u,m}, \\ \psi_{u,n} = \widehat{\mathbf{v}}_{u,n}^H \boldsymbol{\Lambda}_u (\mathbf{I}_{N_u} + \boldsymbol{\Xi}_u \boldsymbol{\Lambda}_u)^{-1} \widehat{\mathbf{v}}_{u,n}, \end{cases} \quad (31)$$

where $\widehat{\mathbf{v}}_{u,m}$ is the m th column of $\widehat{\mathbf{V}}_u$ and $\widehat{\mathbf{u}}_{u,n}$ is the n th column of $\widehat{\mathbf{U}}_u$. The detailed procedure of the DE method is presented in **Algorithm 4**.

Algorithm 4 Deterministic Equivalent Method

Input: The power allocation matrices $\boldsymbol{\Lambda}_u$, $\forall u \in \mathcal{U}$, the right singular matrix $\bar{\mathbf{V}}_2$ and threshold ϵ .

- 1: **for** $u = 1$ to U **do**
- 2: Initialize the iteration index $\ell = 0$ and $\boldsymbol{\psi}_u^{(\ell)}$.
- 3: **repeat**
- 4: Set $\ell = \ell + 1$.
- 5: **for** $m = 1$ to M **do**
- 6: Calculate $\gamma_{u,m}^{(\ell)}$ by (31) with $\boldsymbol{\psi}_u^{(\ell-1)}$.
- 7: **end for**
- 8: Obtain: $\boldsymbol{\gamma}_u^{(\ell)} = [\gamma_{u,1}^{(\ell)}, \gamma_{u,2}^{(\ell)}, \dots, \gamma_{u,M}^{(\ell)}]^T$.
- 9: **for** $n = 1$ to N_u **do**
- 10: Calculate $\psi_{u,N_u}^{(\ell)}$ by (31) with $\boldsymbol{\gamma}_u^{(\ell)}$.
- 11: **end for**
- 12: Obtain: $\boldsymbol{\psi}_u^{(\ell)} = [\psi_{u,1}^{(\ell)}, \psi_{u,2}^{(\ell)}, \dots, \psi_{u,N_u}^{(\ell)}]^T$.
- 13: **until** $\left\| \boldsymbol{\psi}_u^{(\ell)} - \boldsymbol{\psi}_u^{(\ell-1)} \right\|_{\text{F}} \leq \epsilon$
- 14: Use $\boldsymbol{\psi}_u^{(\ell)}$ and $\boldsymbol{\gamma}_u^{(\ell)}$ to calculate $\boldsymbol{\Xi}_u$ and $\boldsymbol{\Psi}_u$ with (30).
- 15: **end for**
- 16: Set $\boldsymbol{\gamma}_u = \boldsymbol{\gamma}_u^{(\ell)}$ and $\boldsymbol{\psi}_u = \boldsymbol{\psi}_u^{(\ell)}$, $\forall u \in \mathcal{U}$, and use them to calculate R_{DE} in (29).

Output: The DE sum-rate R_{DE} and auxiliary variables $\boldsymbol{\psi}_u$, $\boldsymbol{\gamma}_u$, $\boldsymbol{\Xi}_u$, $\boldsymbol{\Psi}$, $\forall u \in \mathcal{U}$.

By adopting the DE method, problem $\bar{\mathcal{P}}_3$ is recast as

$$\bar{\mathcal{P}}_4 : \quad \max_{\boldsymbol{\Lambda}} \quad \frac{R_{\text{DE}}(\boldsymbol{\Lambda})}{W(\boldsymbol{\Lambda})} \quad (32a)$$

$$\text{s.t.} \quad \text{tr} \{ \boldsymbol{\Lambda}_u \} \leq P_{\text{max}}, \boldsymbol{\Lambda}_u \succeq \mathbf{0}, \boldsymbol{\Lambda}_u \text{ diagonal}, \forall u \in \mathcal{U}. \quad (32b)$$

In $\bar{\mathcal{P}}_4$, $R_{\text{DE}}(\mathbf{\Lambda})$ and $W(\mathbf{\Lambda})$ are functions of $\mathbf{\Lambda}$, denoting the asymptotic SE in (29) and the power consumption in the denominator of (27a), respectively. Since variables $\mathbf{\Lambda}$ and $\boldsymbol{\psi}$ are mutually affected, each time $\mathbf{\Lambda}$ is updated, $\boldsymbol{\psi}$ need to be updated by the new $\mathbf{\Lambda}$.

3) *Transmit Power Allocation at Users*: Problem $\bar{\mathcal{P}}_4$ is a classical concave-convex fractional program, so we invoke Dinkelbach's transform to convert it to a convex problem. Specifically, problem $\bar{\mathcal{P}}_4$ is reformulated as

$$\bar{\mathcal{P}}_5 : \quad \arg \max_{\mathbf{\Lambda}, \eta_2} \quad R_{\text{DE}}(\mathbf{\Lambda}) - \eta_2 W(\mathbf{\Lambda}), \quad (33a)$$

$$\text{s.t.} \quad \text{tr} \{ \mathbf{\Lambda}_u \} \leq P_{\text{max}}, \quad \mathbf{\Lambda}_u \succeq \mathbf{0}, \quad \mathbf{\Lambda}_u \text{ diagonal}, \quad \forall u \in \mathcal{U}, \quad (33b)$$

where η_2 is an auxiliary variable. Problem $\bar{\mathcal{P}}_5$ can be efficiently tackled by optimizing $\mathbf{\Lambda}$ and η_2 in an alternating manner. When η_2 is randomly given, the optimal $\mathbf{\Lambda}$ can be obtained by convex optimization techniques [34]. When $\mathbf{\Lambda}$ is given, the optimal solution to η_2 is obtained by

$$\eta_2^* = \frac{R_{\text{DE}}(\mathbf{\Lambda})}{W(\mathbf{\Lambda})}. \quad (34)$$

The optimization process of $\bar{\mathcal{P}}_5$ is similar to **Algorithm 1**. The main difference from **Algorithm 1** is that the optimization process of $\bar{\mathcal{P}}_5$ adopts an asymptotic SE expression, due to lacking the instantaneous CSI. In addition, in $\bar{\mathcal{P}}_5$ we need to consider the interaction between $\mathbf{\Lambda}$ and $\boldsymbol{\psi}$, i.e., each time $\mathbf{\Lambda}$ is updated, $\boldsymbol{\psi}$ must be updated to ensure the asymptotic SE (29) is valid.

C. Optimization of the DMAs Weight Matrix

1) *Optimization of the Unconstrained Weight Matrix*: If the transmit covariance matrices are fixed, the denominator of the objective function in $\bar{\mathcal{P}}_1$ is a constant. Hence, when optimizing \mathbf{Q} with a given \mathbf{P} , we only analyze the numerator of (22a) and ignore the denominator for clarity. By applying the projection matrix property, DE method and *Proposition 2*, the numerator of (22a) is approximated by (29). To maximize (29) with a given $\mathbf{\Lambda}$, we optimize the variable $\bar{\mathbf{V}}_2$ and the auxiliary variable $\boldsymbol{\psi}$ in an iterative manner. When optimizing $\bar{\mathbf{V}}_2$ with a given $\boldsymbol{\psi}$, only the second term of $R_{\text{DE}}(\mathbf{\Lambda})$, $\log_2 |\mathbf{I}_K + \boldsymbol{\Psi}|$, is affected by $\bar{\mathbf{V}}_2$, and the effect on the first and third terms of $R_{\text{DE}}(\mathbf{\Lambda})$ can be removed [37]. Therefore, when $\boldsymbol{\psi}$ is given, we only consider the optimization of the second term, $\log_2 |\mathbf{I}_K + \boldsymbol{\Psi}|$, with respect to $\bar{\mathbf{V}}_2$, and the corresponding

problem without constraint (22b) is formulated as

$$\bar{\mathcal{P}}_6 : \quad \max_{\bar{\mathbf{V}}_2} \quad \log_2 \left| \mathbf{I}_K + \frac{1}{\sigma^2} \sum_{u=1}^U \hat{\mathbf{U}}_u \text{diag} \{ \Omega_u \psi_u \} \hat{\mathbf{U}}_u^H \right|, \quad (35)$$

where $\hat{\mathbf{U}}_u = \bar{\mathbf{V}}_2^H \mathbf{U}_u$.

Define $\mathbf{A} \triangleq \frac{1}{\sigma^2} \sum_{u=1}^U \mathbf{U}_u \text{diag} \{ \Omega_u \psi_u \} \mathbf{U}_u^H$, then the objective function in $\bar{\mathcal{P}}_6$ is written as

$$R_{\text{DE},2} = \log_2 \left| \mathbf{I}_K + \bar{\mathbf{V}}_2^H \mathbf{A} \bar{\mathbf{V}}_2 \right|. \quad (36)$$

Since (36) is identical with (12), a similar conclusion can be obtained from *Proposition 1*, i.e., the maximal $R_{\text{DE},2}$ can be obtained by setting $\bar{\mathbf{V}}_2$ as the eigenvectors corresponding to the largest K eigenvalues of \mathbf{A} . By alternately updating $\bar{\mathbf{V}}_2$ and ψ , we can obtain the optimal solution of $\bar{\mathcal{P}}_6$.

2) *Optimization of the Constrained Weight Matrix*: By the SVD, the weight matrix can be written as $\mathbf{Q} = \mathbf{U}_2 \mathbf{D}_2 \mathbf{V}_2^H$. Similar to the instantaneous CSI case, we apply the alternating minimization algorithm to optimize \mathbf{U}_2 , \mathbf{D}_2 , and \mathbf{Q} . The problem formulation and solution are the same as those in Subsection III-D, so we have omitted the detailed description. The alternating minimization algorithm for optimizing \mathbf{Q} with constraint (22b) can be found in **Algorithm 2**.

D. Overall Algorithm and Complexity Analysis

In the above two subsections, we have provided approaches for designing the transmit covariance matrices of the multi- antenna users and the DMAs weight matrix at the BS with statistical CSI. Unlike Section III, we obtain the transmit directions of each user by a closed-form solution, which significantly reduces the number of variables. In addition, we apply the DE method to approximate the ergodic SE, thus further simplifying the optimization process. The overall algorithm to obtain the power allocation matrices of users and the DMAs weight matrix is presented in **Algorithm 5**.

The complexity of **Algorithm 5** depends on the complexity of the AO-based algorithm (i.e., alternately optimizing Λ in problem $\bar{\mathcal{P}}_5$ and $\bar{\mathbf{V}}_2$ in problem $\bar{\mathcal{P}}_6$) and **Algorithm 2** (i.e., alternately optimizing \mathbf{Q} , $\bar{\mathbf{U}}_2$, and $\bar{\mathbf{D}}_2$). For the AO-based algorithm, the per-iteration complexity mainly depends on optimizing Λ by Dinkelbach's transform. The complexity of the DE method in **Algorithm 4** and the closed-form calculation of $\bar{\mathbf{V}}_2$ is very small, thus is ignored for clarity. We assume that there are I_{DK2} iterations for optimizing Λ by Dinkelbach's

Algorithm 5 AO-based Algorithm for EE Maximization with Statistical CSI

Input: Eigenmode channel coupling matrices $\Omega_u, \forall u$, the noise power σ^2 , power consumptions $W_{c,u}, W_{BS}$, and W_S , threshold ϵ .

- 1: Initialize the iteration index $\ell_1 = \ell_2 = \ell_3 = 0$, the system EE $EE^{(\ell_3)}$, the transmit power allocation matrices $\Lambda_u^{(\ell_1)}, \forall u$, the unconstrained right singular matrix $\bar{\mathbf{V}}_2^{(\ell_2)}$.
 - 2: **do**
 - 3: $\ell_3 = \ell_3 + 1$.
 - 4: Obtain $\boldsymbol{\psi}^{(\ell_1+\ell_2)}$ via $\mathbf{V}_2^{(\ell_2)}, \Lambda_u^{(\ell_1)}, \forall u$, and **Algorithm 4**.
 - 5: Obtain $\eta_2^{(\ell_1+\ell_2)}$ via $\boldsymbol{\psi}^{(\ell_1)}, \Lambda_u^{(\ell_1)}, \forall u$, and (34).
 - 6: **repeat**
 - 7: $\ell_1 = \ell_1 + 1$.
 - 8: Obtain $\Lambda_u^{(\ell_1)}$ in $\bar{\mathcal{P}}_5$ with $\boldsymbol{\psi}^{(\ell_1+\ell_2-1)}$ and $\eta_2^{(\ell_1-1)}$.
 - 9: Update $\boldsymbol{\psi}^{(\ell_1+\ell_2)}$ via $\Lambda_u^{(\ell_1)}, \forall u$, and **Algorithm 4**.
 - 10: Update $\eta_2^{(\ell_1)}$ via $\boldsymbol{\psi}^{(\ell_1+\ell_2)}, \Lambda_u^{(\ell_1)}, \forall u$, and (34).
 - 11: **until** $|\eta_2^{(\ell_1)} - \eta_2^{(\ell_1-1)}| \leq \epsilon$
 - 12: **repeat**
 - 13: $\ell_2 = \ell_2 + 1$
 - 14: Update $\bar{\mathbf{V}}_2^{(\ell_2)}$ via $\boldsymbol{\psi}^{(\ell_1+\ell_2-1)}$ and *Proposition 1*.
 - 15: Update $\boldsymbol{\psi}^{(\ell_1+\ell_2)}$ via $\bar{\mathbf{V}}_2^{(\ell_2)}$ and **Algorithm 4**.
 - 16: **until** $\left\| \bar{\mathbf{V}}_2^{(\ell_2)} - \bar{\mathbf{V}}_2^{(\ell_2-1)} \right\|_{\text{F}} \leq \epsilon$
 - 17: Update $EE^{(\ell_3)}$ via $\bar{\mathbf{V}}_2^{(\ell_2)}$ and $\Lambda_u^{(\ell_1)}, \forall u$.
 - 18: **while** $|EE^{(\ell_3)} - EE^{(\ell_3-1)}| \geq \epsilon$
 - 19: Set $\Lambda_u = \Lambda_u^{(\ell_1)}, \forall u$. Obtain the DMAs weights \mathbf{Q} with $\bar{\mathbf{V}}_2^{(\ell_2)}$ and **Algorithm 2**.
- Output:** The DMAs weights \mathbf{Q} , the transmit power allocation matrices $\Lambda_u, \forall u$.
-

transform. Since the number of the variables is $\sum_{u=1}^U N_u$ in each iteration, the complexity of optimizing Λ is estimated as $\mathcal{O}(I_{\text{DK2}}(\sum_{u=1}^U N_u)^p)$, where $1 \leq p \leq 4$ [19]. In addition, we assume that the AO-based algorithm includes I_{AO} iterations, then its complexity can be approximated by $\mathcal{O}(I_{\text{AO}}I_{\text{DK2}}(\sum_{u=1}^U N_u)^p)$. For alternately optimizing $\mathbf{Q}, \bar{\mathbf{U}}_2$, and $\bar{\mathbf{D}}_2$ by **Algorithm 2**, the complexity is estimated as $\mathcal{O}(I_{\text{Q2}}M^3)$, where I_{Q2} denotes the iteration number and $\mathcal{O}(M^3)$ denotes the complexity per iteration. Hence, by exploiting the statistical CSI, the total complexity of the proposed EE maximization algorithm is $\mathcal{O}(I_{\text{AO}}I_{\text{DK2}}(\sum_{u=1}^U N_u)^p + I_{\text{Q2}}M^3)$.

V. NUMERICAL RESULTS

This section provides numerical results to assess the proposed approach for the DMAs-assisted multiuser MIMO uplink transmission. Our simulation adopts the QuaDRiGa normalization channel model, the 3GPP-UMa-NLoS propagation environment for small scale fading [38], and assumes all the channels exhibit the same large scale fading factor as -120 dB [36]. The channel

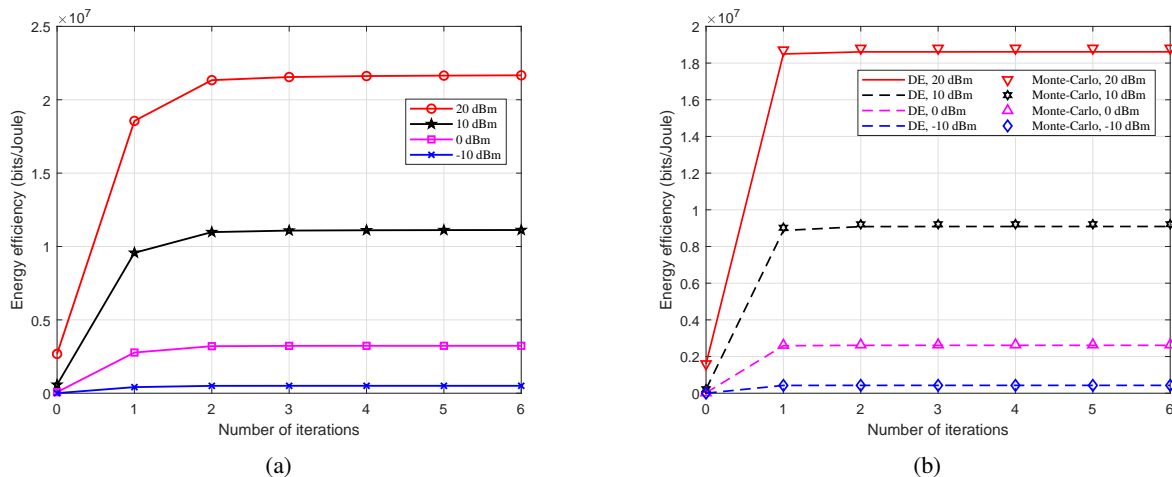


Fig. 2. Convergence performance of the AO-based EE maximization algorithm with different power budgets: (a) instantaneous CSI; (b) statistical CSI.

statistics, $\Omega_u, \forall u$, can be obtained by the existing methods in, e.g., [31]. We set the number of users as $U = 6$ and each user is equipped with 4 antennas, i.e., $N_u = 4, \forall u \in \mathcal{U}$. The antennas of users are placed in uniform linear arrays spaced with half wavelength. We set the number of microstrips as $K = 8$ and each microstrip is embedded with $L = 8$ metamaterial elements. The space between metamaterial elements on the DMAs array is set as 0.2 wavelength. We set the bandwidth as $W = 10$ MHz, set the amplifier inefficiency factor as $\rho = 0.3, \forall u$, and set the noise variance as $\sigma^2 = -96$ dBm. For the power consumption, we set the static circuit power as $W_{c,u} = 20$ dBm, $\forall u$, set the hardware dissipated power at the BS as $W_{BS} = 40$ dBm, and set the static power per microstrip as $W_S = 30$ dBm [19], [39]. Additionally, we choose four classical sets for possible entries of the weight matrix \mathbf{Q} as follows [28]:

- UC: the complex plane, i.e., $\mathcal{Q} = \mathbb{C}$;
- AO: amplitude only, i.e., $\mathcal{Q} = [0.001, 5]$;
- BA: binary amplitude, i.e., $\mathcal{Q} = \{0, 0.1\}$;
- LP: Lorentzian-constrained phase, i.e., $\mathcal{Q} = \{\frac{1+e^{j\phi}}{2} : \phi \in [0, 2\pi]\}$.

A. Convergence Performance

The convergence performance of the proposed AO-based algorithm in the instantaneous CSI case (i.e., alternately designing \mathbf{P} in \mathcal{P}_4 and the unconstrained $\bar{\mathbf{V}}_2$ in \mathcal{P}_2) and the statistical CSI case (i.e., alternately optimizing Λ in problem $\bar{\mathcal{P}}_5$ and $\bar{\mathbf{V}}_2$ in problem $\bar{\mathcal{P}}_6$) under different

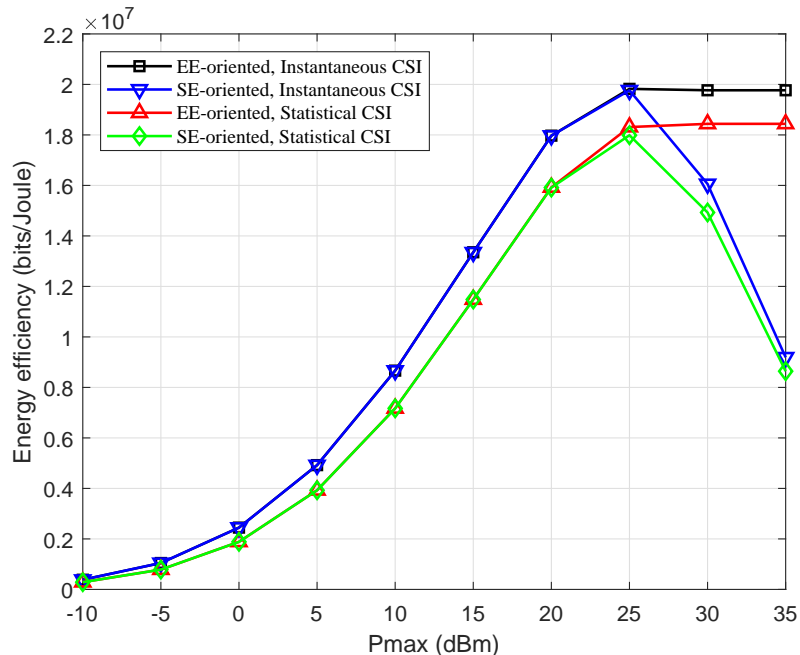


Fig. 3. EE performance comparison between the instantaneous and statistical CSI cases versus the transmit power budget in both the SE- and EE-oriented approaches.

transmit power budgets are respectively presented in Fig. 2(a) and Fig. 2(b). For both cases, the proposed EE maximization algorithms converge at a rapid rate for different power budgets. Besides, Fig. 2(b) verifies the accuracy of the asymptotic SE expression. The gap between the DE- and Monte-Carlo-based results is negligible. Thus, we confirm that adopting the DE method is valid and computationally efficient for resource allocation in the DMAs-assisted MIMO communications with statistical CSI.

B. EE Performance Comparison Between Instantaneous and Statistical CSI Cases

In this subsection, we compare the EE performance of the DMAs-assisted communications between the instantaneous and statistical CSI cases in the EE- and SE-oriented approaches, respectively. As mentioned in Sections III and IV, when the constant $\xi_u, \forall u$, is set as zero in problem \mathcal{P}_1 or $\bar{\mathcal{P}}_1$, the EE maximization problem \mathcal{P}_1 or $\bar{\mathcal{P}}_1$ reduces to the SE maximization one. The corresponding algorithm is referred to as “SE-oriented”.

In Fig. 3, the DMAs weights are chosen from the complex-plane set. We compare the EE performance of the DMAs-assisted uplink system versus the power budget P_{\max} between the instantaneous and statistical CSI cases. As expected, the EE performance is better when the

instantaneous CSI can be perfectly known in both the EE- and SE-oriented approaches. We also observe that the EE performance based on the statistical CSI is quiet close to that based on the instantaneous CSI. Note that, the optimization process in the statistical CSI case is more computationally efficient than the instantaneous CSI one. Thus, in our DMAs-assisted communication scenario, the statistical CSI is a good substitute for the instantaneous CSI to maximize the system EE. In addition, Fig. 3 shows that the EE performance of both EE- and SE-oriented approaches are almost identical in low and medium power regions. This is because in these power budget regions, the circuit and dynamic power consumption dominates the overall power consumption. It also can be observed that the EE performance of the EE-oriented approach remains a constant while that of the SE-oriented one continues to deteriorate in the high power budget region. This phenomenon can be explained as follows. In the EE-oriented approach, there exists a saturation point of the optimal transmit power for maximizing the EE and any power exceeds this threshold is redundant. In the SE-oriented approach, the EE maximization always uses the full-power budget, thus resulting in the degradation of the EE performance in the high power budget region.

C. EE Performance Comparison with Other Baselines

This subsection aims to compare the EE performance between the DMAs- and convectional antennas-assisted systems with fully digital and hybrid A/D architectures. We firstly illustrate the EE models of the conventional antennas-assisted systems for both architectures.

1) *EE Model of Fully Digital Architecture*: The fully digital architecture-based system has M conventional antennas spaced with half wavelength at the BS. The M antenna elements are placed in a uniform planar array and each element is connected with an independent RF chain [40]–[42]. For the case with instantaneous CSI, the achievable EE is given by

$$EE_C = B \frac{\log_2 \left| \mathbf{I}_M + \frac{1}{\sigma^2} \sum_{u=1}^U \mathbf{G}_u \mathbf{P}_u \mathbf{G}_u^H \right|}{\sum_{u=1}^U (\xi_u \text{tr} \{ \mathbf{P}_u \} + W_{c,u}) + W_{BS} + MW_S}. \quad (37)$$

In (37), we use similar notations ξ_u^{-1} , $\text{tr} \{ \mathbf{P}_u \}$, $W_{c,u}$, W_S , and W_{BS} as the EE model in (8). The major difference from (8) is that W_S is multiplied by M in (37) as the number of the required RF chains is equal to the number of antenna elements in the fully digital architecture. In addition, for the case with statistical CSI, a similar EE model can be obtained.

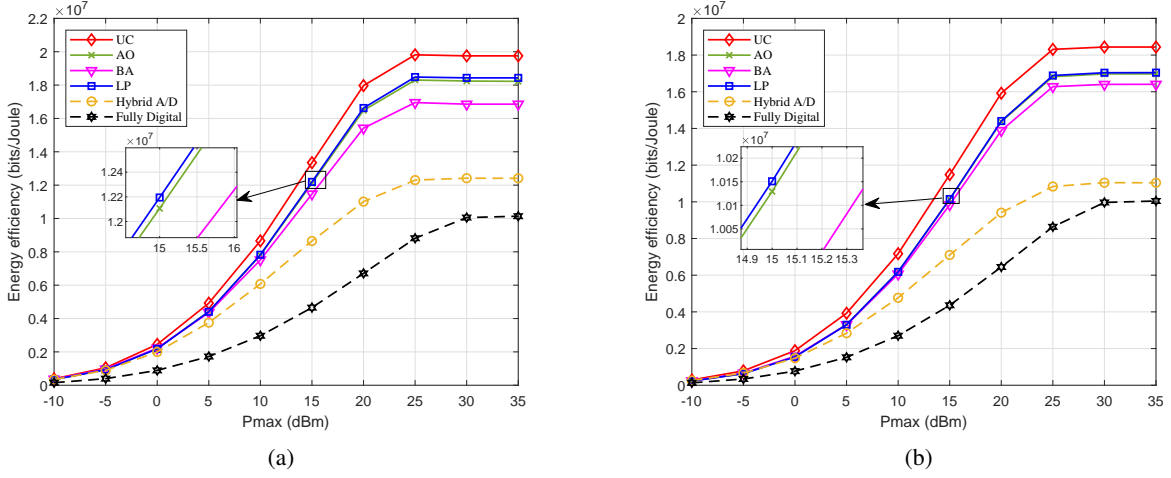


Fig. 4. EE performance comparison between the DMAs- and conventional antennas-assisted systems: (a) instantaneous CSI; (b) statistical CSI.

2) *EE Model of Hybrid A/D Architecture*: To further verify the EE advantages brought by the deployment of DMAs, we compare the DMAs-assisted transmission with the fully-connected hybrid A/D architecture [43]. For the case with instantaneous CSI, the corresponding EE is given by

$$EE_{AD} = B \frac{\log_2 \left| \mathbf{I}_U + \frac{1}{\sigma^2} \sum_{u=1}^U \mathbf{R}_n^{-1} \mathbf{W}^H \mathbf{G}_u \mathbf{P}_u \mathbf{G}_u^H \mathbf{W} \right|}{\sum_{u=1}^U (\xi_u \text{tr} \{ \mathbf{P}_u \} + W_{c,u}) + W_{BS} + KW_S + KMW_p}. \quad (38)$$

In (38), $\mathbf{R}_n = \mathbf{W}^H \mathbf{W}$ where $\mathbf{W} \in \mathbb{C}^{M \times K}$ denotes a hybrid combiner composed of an RF combiner $\mathbf{W}_{RF} \in \mathbb{C}^{M \times K}$ and a baseband combiner $\mathbf{W}_{BB} \in \mathbb{C}^{K \times K}$ at the BS, i.e., $\mathbf{W} = \mathbf{W}_{RF} \mathbf{W}_{BB}$. The RF combiner \mathbf{W}_{RF} is constrained by $|\mathbf{W}_{RF}(i, j)| = 1$ ($i, j \in \{1, 2, \dots, K\}$). In addition, KMW_p denotes the power consumed by the phase shifters, which is the major difference of the power consumption between the fully-connected A/D hybrid and DMAs-assisted transmissions. With the hybrid A/D combining circuitry, the large demand on the RF chains can be greatly reduced compared with the fully digital architecture. In addition, the statistical CSI case can be similarly modeled.

3) *EE Performance Comparison*: In Fig. 4, we compare the EE performance between the DMAs- and conventional antennas-assisted systems for both the instantaneous and statistical CSI cases. We choose the fully digital and fully-connected hybrid A/D architectures at the BS for the conventional antennas-assisted systems as the comparison baseline, whose EE models

are shown above. Referring to [5], we assume that the power consumed by a phase shifter is 30 mW in the hybrid A/D architecture, i.e., $W_p = 30$ mW. Since the EE maximization problem of the fully digital architecture is similar to \mathcal{P}_1 or $\bar{\mathcal{P}}_1$, it can be addressed by Dinkelbach's transform. Similarly, we adopt the AO method to address the EE maximization problem with the hybrid A/D architecture. In particular, we adopt Dinkelbach's transform to optimize the transmit covariance matrices of users and the approach proposed in [5] to optimize the RF and baseband combiners at the BS.

From Fig. 4, we can observe that the EE performance based on DMAs is superior to that based on the conventional fully digital architecture, especially in the high power budget region. This is attributed to the decreased demand on the RF chains at the DMAs-based BSs. Moreover, the EE performance of the DMAs-based system is notably better than that of the fully-connected hybrid A/D one. This is due to that the hybrid A/D architecture requires additional power to support the numerous phase shifters while DMAs do not need any additional circuitry to implement the signal processing in the analog domain. Besides, as expected, the EE performance of the hybrid A/D architecture is better than that of the fully digital architecture, which follows from the less requirement on RF chains in the hybrid A/D architecture than that in the fully digital architecture. In addition, we can find that the EE saturation point of the DMAs-based system is shifted to the left compared with the fully digital one. This is because the DMAs-based systems consume much less dynamic power with the reduced demand on RF chains. For a lower dynamic power, the required transmit power will decrease to become the dominant term of the whole power consumption.

Comparing the four classical sets of DMAs weights mentioned above, we can find that their corresponding curves scale similarly versus the transmit power budget. Among the four cases, the system EE of the complex plane case performs the best, which is attributed to the fact that the corresponding set contains the other three as subsets. We also observe that the EE performance of the continuous-valued amplitude, binary amplitude, and Lorentzian-constrained phase cases are close to the complex plane one. This phenomenon indicates that compared to the system EE in the complex plane case, the degradation of the EE performance resulting from narrowing the sets is almost negligible. It shows the possibility of a simpler implementation to achieve the comparable channel capacity and EE performance with the continuous-valued amplitude, binary amplitude, and Lorentzian-constrained phase sets. In fact, implementing the binary amplitude is much simpler than the others, which makes it a more appealing solution among the four kinds

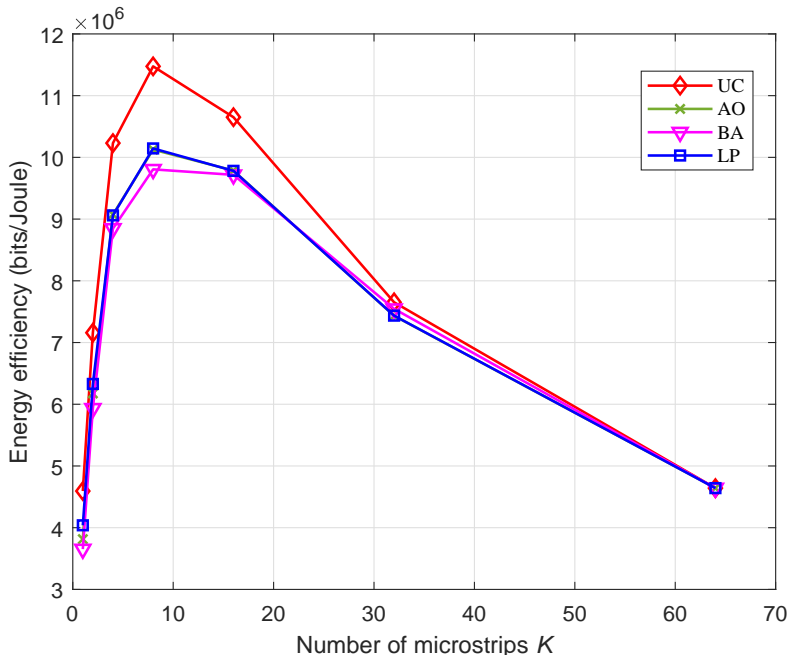


Fig. 5. EE performance comparison with statistical CSI versus the number of microstrips K when the total number of metamaterials is fixed.

for future studies.

D. Effect of Number of Microstrips

In Fig. 5, we evaluate the effects of the number of microstrips on the EE performance of the DMAs-assisted communications. We fix the number of metamaterials to $M = 64$, set the transmit power consumption budget P_{\max} as 15 dBm, and evaluate the EE performance of the DMAs-assisted system for $K \in [1, 64]$. As is shown in Fig. 3, the EE performance based on the statistical CSI is close to that based on the instantaneous CSI, thus we only present the EE performance based on the statistical CSI here and omit the instantaneous CSI case.

From Fig. 5, we note again that the achievable EE performance based on the continuous-valued amplitude, binary amplitude, and Lorentzian-constrained phase cases are close to each other, and closely follow the complex plane case. We can also observe that, for the cases with small K , the EE performance of the DMAs-based system is rapidly improved as the number of microstrips increases. This is because the signal propagation generates attenuation inside the microstrip, which is proportional to the number of metamaterials on a microstrip. Thus, increasing the number of microstrips (i.e., reducing the number of metamaterials on a microstrip) will reduce

the propagation loss and improve the system EE performance. Moreover, in the cases with large K , the EE performance decreases as the number of microstrips increases. This phenomenon can be explained as follows. When the number of microstrips K is large, the metamaterials that can be removed from a microstrip is relatively few, i.e., the reduction of the signal propagation loss is limited. Thus, the corresponding EE improvement is small and limited. Meanwhile, the dynamic power dissipation, which is proportional to the number of microstrips, dominates the total power consumption. As the dynamic power dissipation increases, the EE performance reduces in a rapid and non-negligible rate. The two aspects together lead to a reduction in the EE performance with large K . This observation implies that in practical implementation, we need to strike a balance between the power consumption (proportional to the number of RF chains) and propagation loss (proportional to the number of metamaterials per microstrips) to further improve the EE performance in the DMAs-assisted communications.

VI. CONCLUSION

Our work studied the EE performance optimization of the DMAs-assisted massive MIMO uplink communications by exploiting either instantaneous or statistical CSI. Specifically, we developed a well-structured and low-complexity framework for the transmit covariance design of each user and the DMAs configuration strategy at the BS, including the AO and DE methods, as well as Dinkelbach's transform. Based on our algorithm, the DMAs-assisted communications achieved much higher EE performance gains compared to the conventional large-scale antenna arrays-assisted ones, especially in the high power budget region. The results also showed that the EE performance based on DMAs could be further improved by adjusting the number of microstrips.

REFERENCES

- [1] J. Xu, L. You, G. C. Alexandropoulos, J. Wang, W. Wang, and X. Q. Gao, "Dynamic metasurface antennas for energy efficient uplink massive MIMO communications," in *Proc. IEEE GLOBECOM*, Madrid, Spain, 2021, pp. 1–6.
- [2] V. W. S. Wong, R. Schober, D. W. K. Ng, and L. C. Wang, *Key Technologies for 5G Wireless Systems*. Cambridge, U.K.: Cambridge Univ. Press, 2017.
- [3] T. L. Marzetta, "Massive MIMO: An introduction," *Bell Labs Tech. J.*, vol. 20, pp. 11–22, Mar. 2015.
- [4] J. G. Andrews, S. Buzzi, W. Choi, S. V. Hanly, A. Lozano, A. C. K. Soong, and J. C. Zhang, "What will 5G be?" *IEEE J. Sel. Areas Commun.*, vol. 32, no. 6, pp. 1065–1082, May 2014.
- [5] R. Méndez-Rial, C. Rusu, N. González-Prelcic, A. Alkhateeb, and R. W. Heath, "Hybrid MIMO architectures for millimeter wave communications: Phase shifters or switches?" *IEEE Access*, vol. 4, pp. 247–267, Mar. 2016.

- [6] J. Mo, A. Alkhateeb, S. Abu-Surra, and R. W. Heath, "Hybrid architectures with few-bit ADC receivers: Achievable rates and energy-rate tradeoffs," *IEEE Trans. Wireless Commun.*, vol. 16, no. 4, pp. 2274–2287, Apr. 2017.
- [7] L. You, Y. Huang, D. Zhang, Z. Chang, W. Wang, and X. Q. Gao, "Energy efficiency optimization for multi-cell massive MIMO: Centralized and distributed power allocation algorithms," *IEEE Trans. Commun.*, 2021, to be published, doi:10.1109/TCOMM.2021.3081451.
- [8] P. A. Hoeher and N. Doose, "A massive MIMO terminal concept based on small-size multi-mode antennas," *Trans. Emerging Tel. Tech.*, vol. 28, no. 2, Feb. 2017.
- [9] N. Shlezinger, G. C. Alexandropoulos, M. F. Imani, Y. C. Eldar, and D. R. Smith, "Dynamic metasurface antennas for 6G extreme massive MIMO communications," *IEEE Wireless Commun.*, vol. 28, no. 2, pp. 106–113, Apr. 2021.
- [10] C. Liaskos, S. Nie, A. Tsioliaridou, A. Pitsillides, S. Ioannidis, and I. Akyildiz, "A new wireless communication paradigm through software-controlled metasurfaces," *IEEE Commun. Mag.*, vol. 56, no. 9, pp. 162–169, Sep. 2018.
- [11] M. D. Renzo, M. Debbah, D.-T. Phan-Huy, A. Zappone, M.-S. Alouini, C. Yuen, V. Sciancalepore, G. C. Alexandropoulos, J. Hoydis, H. Gacanin, J. de Rosny, A. Bounceu, G. Lerosey, and M. Fink, "Smart radio environments empowered by reconfigurable AI meta-surfaces: An idea whose time has come," *EURASIP J. Wireless Commun. Netw.*, vol. 2019, p. 129, May 2019.
- [12] C. L. Holloway, E. F. Kuester, J. A. Gordon, J. O'Hara, J. Booth, and D. R. Smith, "An overview of the theory and applications of metasurfaces: The two-dimensional equivalents of metamaterials," *IEEE Antennas Propag. Mag.*, vol. 54, no. 2, pp. 10–35, Apr. 2012.
- [13] C. Pfeiffer and A. Grbic, "Metamaterial huygens' surfaces: Tailoring wave fronts with reflectionless sheets," *Phys. Rev. Lett.*, vol. 110, no. 19, p. 197401, May 2013.
- [14] N. Engheta and R. W. Ziolkowski, *Metamaterials: Physics and Engineering Explorations*. Hoboken, NJ: Wiley-IEEE Press, 2006.
- [15] D. R. Smith, O. Yurduseven, L. P. Mancera, and P. Bowen, "Analysis of a waveguide-fed metasurface antenna," *Phys. Rev. Appl.*, vol. 8, no. 5, Nov. 2017, Art. no. 054048.
- [16] G. C. Alexandropoulos and E. Vlachos, "A hardware architecture for reconfigurable intelligent surfaces with minimal active elements for explicit channel estimation," in *Proc. IEEE ICASSP*, Barcelona, Spain, 2020, pp. 9175–9179.
- [17] L. You, J. Xiong, Y. Huang, D. W. K. Ng, C. Pan, W. Wang, and X. Q. Gao, "Reconfigurable intelligent surfaces-assisted multiuser MIMO uplink transmission with partial CSI," *IEEE Trans. Wireless Commun.*, 2021, to be published, doi:10.1109/TWC.2021.3068754.
- [18] C. Pan, H. Ren, K. Wang, W. Xu, M. Elkashlan, A. Nallanathan, and L. Hanzo, "Multicell MIMO communications relying on intelligent reflecting surfaces," *IEEE Trans. Wireless Commun.*, vol. 19, no. 8, pp. 5218–5233, Aug. 2020.
- [19] C. Huang, A. Zappone, G. C. Alexandropoulos, M. Debbah, and C. Yuen, "Reconfigurable intelligent surfaces for energy efficiency in wireless communication," *IEEE Trans. Wireless Commun.*, vol. 18, no. 8, pp. 4157–4170, Aug. 2019.
- [20] C. Huang, S. Hu, G. C. Alexandropoulos, A. Zappone, C. Yuen, R. Zhang, M. D. Renzo, and M. Debbah, "Holographic MIMO surfaces for 6G wireless networks: Opportunities, challenges, and trends," *IEEE Wireless Commun.*, vol. 27, no. 5, pp. 118–125, Oct. 2020.
- [21] G. C. Alexandropoulos, N. Shlezinger, and P. D. Hougne, "Reconfigurable intelligent surfaces for rich scattering wireless communications: Recent experiments, challenges, and opportunities," *IEEE Commun. Mag.*, 2021, to be published.
- [22] G. C. Alexandropoulos, N. Shlezinger, I. Alamzadeh, M. F. Imani, H. Zhang, and Y. C. Eldar, "Hybrid reconfigurable intelligent metasurfaces: Enabling simultaneous tunable reflections and sensing for 6G wireless communications," *arXiv preprint arXiv:2104.04690*, 2021.

- [23] L. You, J. Xiong, D. W. K. Ng, C. Yuen, W. Wang, and X. Q. Gao, "Energy efficiency and spectral efficiency tradeoff in RIS-aided multiuser MIMO uplink transmission," *IEEE Trans. Signal Process.*, vol. 69, pp. 1407–1421, Mar. 2021.
- [24] M. C. Johnson, S. L. Brunton, J. N. Kutz, and N. B. Kundtz, "Sidelobe canceling for optimization of reconfigurable holographic metamaterial antenna," *IEEE Trans. Antennas Propag.*, vol. 63, no. 4, pp. 1881–1886, Apr. 2015.
- [25] I. Yoo, M. F. Imani, T. Slesman, H. D. Pfister, and D. R. Smith, "Enhancing capacity of spatial multiplexing systems using reconfigurable cavity-backed metasurface antennas in clustered MIMO channels," *IEEE Trans. Commun.*, vol. 67, no. 2, pp. 1070–1084, Feb. 2019.
- [26] H. Wang, N. Shlezinger, Y. C. Eldar, S. Jin, M. F. Imani, I. Yoo, and D. R. Smith, "Dynamic metasurface antennas for MIMO-OFDM receivers with bit-limited ADCs," *IEEE Trans. Commun.*, vol. 69, no. 4, pp. 2643–2659, Apr. 2021.
- [27] H. Wang, N. Shlezinger, S. Jin, Y. Eldar, I. Yoo, M. F. Imani, and D. R. Smith, "Dynamic metasurface antennas based downlink massive MIMO systems," in *Proc. IEEE SPAWC*, Cannes, France, Jul. 2019, pp. 1–5.
- [28] N. Shlezinger, O. Dicker, Y. C. Eldar, I. Yoo, M. F. Imani, and D. R. Smith, "Dynamic metasurface antennas for uplink massive MIMO systems," *IEEE Trans. Commun.*, vol. 67, no. 10, pp. 6829–6843, Oct. 2019.
- [29] A. Zappone, M. Di Renzo, F. Shams, X. Qian, and M. Debbah, "Overhead-aware design of reconfigurable intelligent surfaces in smart radio environments," *IEEE Trans. Wireless Commun.*, vol. 20, no. 1, pp. 126–141, Jan. 2021.
- [30] Q. Wu and R. Zhang, "Towards smart and reconfigurable environment: Intelligent reflecting surface aided wireless network," *IEEE Commun. Mag.*, vol. 58, no. 1, pp. 106–112, Jan. 2020.
- [31] X. Q. Gao, B. Jiang, X. Li, A. B. Gershman, and M. R. McKay, "Statistical eigenmode transmission over jointly-correlated MIMO channels," *IEEE Trans. Inf. Theory*, vol. 55, no. 8, pp. 3735–3750, Sep. 2009.
- [32] A. Zappone and E. Jorswieck, "Energy efficiency in wireless networks via fractional programming theory," *Found. Trends Commun. Inf. Theory*, vol. 11, no. 3-4, pp. 185–396, Jan. 2015.
- [33] C. D. Meyer, *Matrix Analysis and Applied Linear Algebra*. Philadelphia, PA, USA: SIAM, 2000.
- [34] S. Boyd and L. Vandenberghe, *Convex Optimization*. New York, NY, USA: Cambridge Univ. Press, 2004.
- [35] A. Ben-Tal and A. Nemirovski, *Lectures on Modern Convex Optimization: Analysis, Algorithms, and Engineering Applications*. Philadelphia, PA, USA: SIAM, 2001, vol. 2.
- [36] L. You, J. Xiong, X. Yi, J. Wang, W. Wang, and X. Gao, "Energy efficiency optimization for downlink massive MIMO with statistical CSIT," *IEEE Trans. Wireless Commun.*, vol. 19, no. 4, pp. 2684–2698, Apr. 2020.
- [37] C.-K. Wen, S. Jin, and K.-K. Wong, "On the sum-rate of multiuser MIMO uplink channels with jointly-correlated Rician fading," *IEEE Trans. Commun.*, vol. 59, no. 10, pp. 2883–2895, Oct. 2011.
- [38] S. Jaeckel, L. Raschkowski, K. Borner, and L. Thiele, "QuaDRiGa: A 3-D multi-cell channel model with time evolution for enabling virtual field trials," *IEEE Trans. Antennas Propag.*, vol. 62, no. 6, pp. 3242–3256, Jun. 2014.
- [39] S. He, Y. Huang, S. Jin, and L. Yang, "Coordinated beamforming for energy efficient transmission in multicell multiuser systems," *IEEE Trans. Commun.*, vol. 61, no. 12, pp. 4961–4971, Dec. 2013.
- [40] T. L. Marzetta, "Noncooperative cellular wireless with unlimited numbers of base station antennas," *IEEE Trans. Wireless Commun.*, vol. 9, no. 11, pp. 3590–3600, Nov. 2010.
- [41] J. Hoydis, S. ten Brink, and M. Debbah, "Massive MIMO in the UL/DL of cellular networks: How many antennas do we need?" *IEEE J. Sel. Areas Commun.*, vol. 31, no. 2, pp. 160–171, Feb. 2013.
- [42] L. You, X. Chen, X. Song, F. Jiang, W. Wang, X. Q. Gao, and G. Fettweis, "Network massive MIMO transmission over millimeter-wave and terahertz bands: Mobility enhancement and blockage mitigation," *IEEE J. Sel. Areas Commun.*, vol. 38, no. 12, pp. 2946–2960, Dec. 2020.
- [43] S. S. Ioushua and Y. C. Eldar, "A family of hybrid analog-digital beamforming methods for massive MIMO systems," *IEEE Trans. Signal Process.*, vol. 67, no. 12, pp. 3243–3257, Jun. 2019.